Available online at www.sciencedirect.com
ScienceDirect
Thin Solid Films 515 (2006) 382 – 388
www.elsevier.com/locate/tsf

Ti–Zr–V non-evaporable getter films: From development to large scale production for the Large Hadron Collider

P. Chiggiato *, P. Costa Pinto

CERN, European Organization for Nuclear Research 1211, Geneva 23, Switzerland

Available online 23 January 2006

Abstract

Non-evaporable getter (NEG) alloys after dissolution of their native oxide layer into the bulk are able to pump most of the gases present in ultra-high vacuum systems. The dissolution process, commonly called activation, is obtained by heating in vacuum. NEG materials can be sputter-deposited as a thin film on the inner wall of a vacuum chamber, transforming it from a source of gas into an effective pump. The most significant advance in the development of NEG films was the discovery of a very low activation temperature (180 °C for 24 h heating) in a large range of compositions of the Ti–Zr–V system. This favourable property was correlated with nanometric grain size of the film (about 3 to 5 nm).

In addition to pumping, NEG films lead to reduced induced gas desorption and secondary electron yields. As a consequence, Ti–Zr–V films provide the optimum solution to most of the problems encountered in vacuum systems of modern particle accelerators for high energy physics and for synchrotron radiation facilities. In the near future the most significant benchmark for Ti–Zr–V films will be the Large Hadron Collider (LHC) presently under construction at CERN, where about 6 km of beam pipe are being coated. A dedicated magnetron sputtering facility has been built to cope with the high number of vacuum chambers (about 1200) and the tight production schedule.

PACS: 07.30.-t; 07.85.Qe
Keywords: NEG coatings; Getters; Pumping; Ultra-high vacuum; Particle accelerators; LHC

1. Introduction

The wish of any UHV user to transform the wall of vacuum systems from a source of gas into a pumping surface has become a reality after a passionate development conducted at CERN between 1995 and 2002 [1]. This advance was obtained by ex situ sputter-coating the whole inner surface of vacuum chambers with a thin non-evaporable getter (NEG) film. By heating in vacuum (activation), the native oxide layer of such a film is dissolved into the bulk allowing chemisorption of most of the gases present in vacuum systems at room temperature. In this perspective the film coating is considered as an integral part of the vacuum chamber. This technological breakthrough represents the natural evolution of pumping solutions for particle accelerators. In effect, to counteract the more and more limited conductance of beam pipes, distributed pumping is necessary to produce a uniform pressure profile [2]. Linearly distributed ion pumps [3] and NEG strips [4] were used in the past for such application. However, both these lines of attack are demanding in terms of space and a dedicated antechamber is necessary for their integration in the beam pipe.

The activation temperature of the selected coatings must be lower than the maximum temperature allowed for UHV vacuum chambers, namely 400, 250 and 200 °C for those made of stainless steel, copper alloys and aluminium alloys, respectively. The dissolution of the native oxide is possible at such temperatures only if the transfer of oxygen in the solid solution is thermodynamically possible and oxygen diffusion rate in the film is sufficiently fast [5]. It turns out that the key parameters for the choice of NEG coating materials are the oxygen solubility limit, i.e., the maximum concentration of oxygen that can be dissolved in solid solution, and the oxygen diffusivity in the film [5]. With respect to the thermodynamic characteristic, the elements of the fourth group (Ti, Zr, Hf) have a singular behaviour: they show an exceptionally high ability to dissolve oxygen attaining values of concentrations up to 30 at.%. In the nearby groups the solubility limit drops to values well below 1 at.% at temperatures lower than 400 °C (except for V and Sc, about 3 and 1 at.%, respectively) [6]. With regard to the kinetic parameter, an enhanced diffusion can be achieved in the elements of the fourth group by adding other elements that

* Corresponding author. Tel.: +41 22 7676387; fax: +41 22 7678380.
E-mail address: paolo.chiggiato@cern.ch (P. Chiggiato).

0040-6090/$ - see front matter © 2005 Elsevier B.V. All rights reserved.
doi:10.1016/j.tsf.2005.12.218

either enlarge the lattice space (increased bulk diffusivity) [7,8] or reduce the grain size and, as a result, increase the transport of oxygen through the grain boundaries. The latter approach was successfully verified for Ti–Zr–V alloys where compositions with very low activation temperatures are unambiguously associated with grains of nanometric size (about 3 to 5 nm) [5,9]. The activation of these films can be obtained by heating at 180 °C for 24 h, which renders Ti–Zr–V films compatible with all the substrate materials used in vacuum technology [10].

The properties of Ti–Zr–V films have been studied to verify their suitability with a particle accelerator environment [11,12]. The positive outcomes of this investigation have lead to important applications to some high-energy physics [13] and synchrotron radiation facilities [14]. However, by far the most significant benchmark for such films will be the Large Hadron Collider (LHC) presently under construction at CERN, where about 6 km of beam pipe (about 1200 vacuum chambers) are being coated.

2. General properties of Ti–Zr–V films

Ti–Zr–V films are produced by magnetron sputtering and most of the know-how in the coating process comes from the experience acquired with thin film Nb coating for superconducting RF cavities [15,16].

Films of different compositions were produced [5,9] on coupon samples made of different materials by means of a dedicated system equipped with a planar sputtering source for each of the three elements. The samples were characterised by Auger Electron Spectroscopy (AES) [17] and their performances ranked by the ratio between the intensity of metallic and oxide Zr lines after a defined thermal cycle (200 °C for 1 h). In addition Energy Dispersive X-ray (EDX), X-Ray Diffraction (XRD) and Transmission Electron Microscopy (TEM) were applied to probe compositions and crystal structures [5].

The results have indicated that the nanometric grain size along with the fast oxide layer dissolution are obtained for a large range of compositions characterised by a Ti concentration lower than about 45%. Other studies carried out by X-ray Photoelectron Spectroscopy (XPS) and Secondary Ion Mass Spectroscopy (SIMS) have clarified the activation mechanism of these alloys [18–20]; in particular they have shown that V is the first of the three metals to be reduced as it could have been expected by the comparison of the three oxide formation enthalpies. The large domain of compositions where the dissolution is facilitated allows the production of simple and quite inexpensive cathodes for the coating of vacuum chambers: the three elemental wires are intertwisted to form a braid which is positioned along the tube axis for the coating process. In this configuration the actual composition is Ti 30–Zr 30–V 40 at.% for 3 mm diameter wires.

The nature of the substrate does not influence the oxide dissolution process of the Ti–Zr–V film [21]. This is not the case for morphology: such a film coated on smooth copper and stainless steel is smooth and compact, whereas on aluminium alloys and beryllium a cauliflower structure is formed. Nevertheless, the most spectacular effect on film morphology is played by the substrate temperature during coating [22]: for temperatures equal to or higher than 250 °C the film grows with a columnar and granular structure resulting in an increase of the surface area of a factor of about 10. A higher substrate roughness can further enhance the film surface area. Moreover, the substrate temperature during coating should not be higher than 300 °C since this produces an increase of the grain size which leads to a higher activation temperature [22].

The content of H in the film after coating is about 0.1 at.% which is very close to the value measured for Nb films coated in similar configurations [23]. The content of the discharge gas trapped in the film depends at first approximation on the momentum exchange between energetic ions impinging on the cathode and the cathode atoms [24]. Therefore, lighter ions hitting heavy cathode atoms are reflected with higher energy and get more easily implanted in the growing film. The practical consequence is that Kr is less implanted than Ar in Ti–Zr–V films. This result was verified experimentally by ablating the film in a vacuum system, on less than 0.1 mm^2, by an excimer laser [25]. The evaporation of the film frees the trapped gas whose quantity is evaluated by a calibrated mass spectrometer [26,27]. Discharge gas content is strongly dependent on many parameters, for instance cathode voltage, pressure, substrate-cathode distance and substrate temperature. In a film deposited on a vacuum chamber, about 100 and 1000 at. ppm were measured for Kr and Ar, respectively, for typical coating parameters (−500 V polarisation, 10^{-2} Torr discharge gas pressure, 100 °C substrate temperature) and for a distance of about 5 cm between the axial cathode and the substrate.

3. Vacuum properties of Ti–Zr–V films

3.1. Pumping speed

Ti–Zr–V films are used as pumps; for that reason their main functional characteristic is the pumping speed for the gases present in UHV systems, i.e., H_2, CO, CO_2, H_2O and N_2 and O_2 in case of leaks. NEG materials do not pump noble gases. Negligible pumping is also provided for CH_4 due to the high dissociation energy for this molecule at metal surfaces [28,29]; an upper limit for the CH_4 sticking probability at room temperature is 10^{-6} [30]. A similar result was obtained at CERN for Ti–Zr–V.

Pumping speeds are frequently expressed in terms of sticking probabilities, namely the ratio of the rate of chemically adsorbed molecules to the total rate of molecules incident on the surface.

The pumping characteristics of Ti–Zr–V films are similar to those obtained for bulk NEG materials of different chemical composition [31,32]. Sticking probability depends on the gas specie, on the surface coverage, i.e., on quantity of gas already pumped, and on the NEG surface roughness. Typical values are reported in Table 1. The sticking probabilities of homonuclear molecules are at least about a factor of 10 lower than that of CO. The pumping speed of all the gases, except that of H_2, decreases as the coverage of the same gas increases. H_2, after dissociation on the surface, can diffuse in the film bulk; as a consequence its pumping speed displays

Table 1
Summary of the some functional properties of Ti–Zr–V film coatings

		H_2	CO	N_2	CH_4
Maximum sticking probability	Smooth	8×10^{-3}	0.7	1.5×10^{-2}	
	Rough	3×10^{-2}	0.9	3.0×10^{-2}	
Surface capacity [molecules cm^{-2}]	Smooth		8×10^{14}	1.5×10^{14}	
	Rough		8×10^{15}	1.5×10^{15}	
Electron stimulated desorption yields [molecules per impinging electron]	Electron energy=500 eV negligible dose	2×10^{-4}	1×10^{-4}		5×10^{-6}
Photon stimulated desorption yields [molecules per impinging photon]	E_c=194 eV [51] negligible dose, normal incidence	3×10^{-6}	$<2\times10^{-8}$		$<3\times10^{-8}$
	E_c=4.5 KeV [41,42] 10^{21} ph m^{-1} 10 mrad incidence	1.5×10^{-5}	$<10^{-5}$		2×10^{-7}

Pumping speed and gas capacity are referred to film coated at 100 °C (smooth) and 250 °C (rough). Electron and photon desorption yields are reported only for smooth films. Pumping speed and gas capacity can be improved by increasing the substrate roughness.

a much smaller decrease with the pumped quantity, but it is dependent on the rate of arrival of the molecules. The surface capacity of CO and CO_2 is of the same order as the number of atoms on the surface, i.e., about 10^{15} molecules cm^{-2} for a smooth surface. Therefore the surface capacity can be increased by increasing the film surface roughness as obtained by coating at high temperature as shown in Fig. 1-a and -b. The maximum surface coverage for N_2 is about 5 times lower than that of CO since the chemical adsorption of this molecule needs several free adsorption sites [33]. On the contrary, the maximum surface coverage for H_2O and O_2 is about 5 times larger than that for CO because, after surface dissociation, underlayer penetration [33,34] of atomic oxygen can occur. An increased film surface roughness not only expands the surface gas capacity, it also enhances the sticking probability due to possible molecule-surface multiple impingement.

For porous Ti–Zr–V films, as those coated at temperature higher than 250 °C, for high CO and CO_2 coverage, the pumping speeds decrease as the inverse of the pumped quantity. This behaviour can be understood by considering that the molecules have to pass through a saturated porous layer before reaching free adsorption sites. The saturated layer has a molecular conductance which decreases as the inverse of its thickness, namely as the inverse of the pumped quantity [31].

The presence of a given gas influences the film pumping speed for another gas as shown in Fig. 1-a and -b for N_2 and H_2 on a CO charged film surface. H_2 does not affect the pumping speed of the other gases since it diffuses inside the material, while N_2 has a limited influence on the pumping of H_2 and CO as a result of its underlayer adsorption [21,32,35].

3.2. Ultimate pressure intrinsic limitations

Total pressures in the low 10^{-13} Torr range have been reproducibly measured in Ti–Zr–V coated vacuum chambers [36]. It has been shown that this limitation is not due to any film features, but to the outgassing of the gauge employed (of the order of 10^9 molecules s^{-1}) and to the NEG pumping speed available at the gauge position. The film characteristics that could limit the ultimate pressure are outgassing of species which are not pumped by NEG, namely the discharge gas and methane, and hydrogen dissociation pressure.

Kr and CH_4 outgassing rates have been measured for several Ti–Zr–V coated vacuum chambers made of different materials [37]. The Kr outgassing rates at room temperature are of the order of 10^{-18} Torr l s^{-1} cm^{-2} ($\approx$30 molecules s^{-1} cm^{-2}) or lower. The same value at the temperature of activation never exceeds 10^{-13} Torr l s^{-1} cm^{-2} ($\approx3\times10^6$ molecules s^{-1} cm^{-2}). The Kr desorption energy is 21±1 Kcal mol^{-1} and it does not depend on the substrate nature. The quantity of Kr released by the film during a 200 °C heating for 24 h is negligible in comparison with the expected trapped quantity of the same gas in the film, i.e., about 1000 times lower [37]. The measurement of the CH_4 outgassing rates could be affected by the presence of UHV gauges which can produce a relevant quantity of this gas. To overcome this problem, accumulation of the desorbed gas in a volume without gauges is mandatory. The evaluation of the accumulated quantity is usually obtained by expanding the gas in a chamber equipped with a calibrated gas analyser. With such a method, values of the order of 10^{-18} Torr l s^{-1} cm^{-2} ($\approx$30 molecules s^{-1} cm^{-2}) were measured at room temperature after activation. The practical consequence of these extremely low outgassing values is that auxiliary pumps (ion, turbomolecular or cryogenic pumps) with very low pumping speed for these gases are sufficient for attaining very low pressures in Ti–Zr–V coated chambers.

The Sieverts' law for the H_2 dissociation pressure of Ti–Zr–V films was experimentally evaluated [38] and it is expressed by the following relation:

$$\log(P_{H_2}) = 2\cdot\log(x_H) + 14.2 - \frac{8468}{T}$$

where x_H is the fraction of atomic hydrogen in the film, P_{H2} is the dissociation pressure in Torr and T the temperature in K. It comes out that for the expected H content the dissociation pressure is negligible at room temperature, but its value becomes about 10^{-10} Torr at the lowest possible activation temperature, namely 180 °C.

3.3. Induced desorption

In an accelerator vacuum system, the gas load is not only defined by the thermal outgassing. In most of the modern high-energy and synchrotron radiation facilities, the inner surfaces

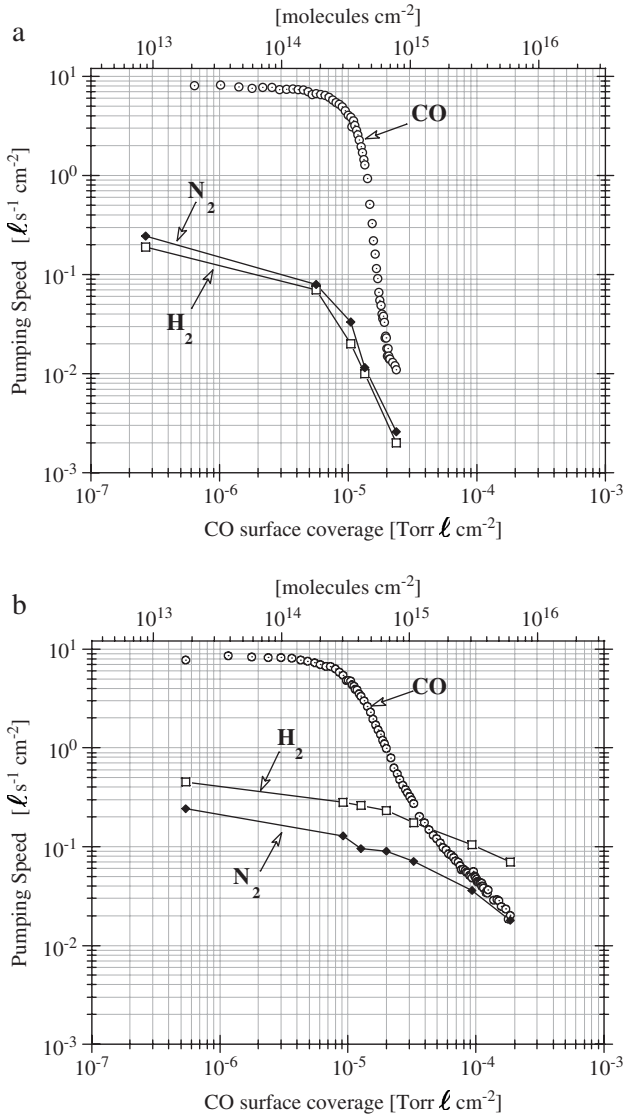

Fig. 1. a and b Pumping speed of CO, N_2 and H_2 as a function of the quantity of CO adsorbed for Ti–Zr–V samples coated at 100 (a) and 300 °C (b). For the porous film and for high gas coverage, the ratio of the pumping speeds for the three gases equals the ratio of the molecular conductances. The pumping speeds can be converted into sticking factors by dividing their values by the unit surface molecular conductance at room temperature, i.e., 44 l s^{-1} cm^{-2} for H_2 and 11.6 l s^{-1} cm^{-2} for CO and N_2.

of the beam pipes are bombarded by electrons, photons and ions which induce the desorption of gas molecules [39]. The experimental data available shows that the source of such a gas load could be the oxide layer. As a consequence, a lower desorption yield (molecules desorbed per impinging particle) is expected for NEG films since their oxide layer is dissolved during activation. This expectation has been corroborated by several measurements. The measured electron desorption yields for H_2 and CO are at least 10 times lower than those for stainless steel; that for CH_4 at least 100 times lower [40]. The same features were measured for photon induced desorption for critical energies in the range between 20 eV and 20 KeV [12,14,41,42]. Data for ion induced desorption for low impinging energy (from 100 eV to 100 KeV) are lacking. However encouraging results have been obtained at CERN for very high energy Pb ion collisions at 4.2 MeV/nucleon [43].

3.4. Secondary electron yield

In particle accelerators secondary electrons can gain kinetic energy from positive charged beams and, by colliding on the facing surface, release other electrons. A positive feedback process is possible if the secondary electron yield (SEY) and the frequency of the accelerated particle bunches are higher than well defined thresholds [44]. The intense electron bombardment provokes localised pressure bumps which are detrimental for beam lifetime, luminosity and thermal load in the cold bore of superconductive magnets. The SEY can be reduced by removing the oxide layer as it is the case for the induced desorption yields. Dedicated measurements [45] have shown that the SEY of activated Ti–Zr–V films is lower than that for traditional structural materials at equal electron dose. The SEY at the peak maximum for the NEG film is about 1.1–1.2, whereas for stainless steel and copper it reaches values of about 2 at negligible electron doses. This property is of paramount importance for high-energy modern accelerators [46].

3.5. Performance deterioration: ageing of Ti–Zr–V films

In many applications, vacuum chambers are frequently exposed to air and, as a consequence, Ti–Zr–V coatings undergo several venting–activation cycles. Since the film thickness is typically about 1 μm and the maximum quantity of oxygen that can be dissolved in the film is limited, a deterioration of the film performances is expected [11]. The drift of the film characteristics were probed by injecting H_2 in 2 m long, 3.4 cm diameter, stainless steel pipes and evaluating the sticking probability for such a gas. The results show a gradual decrease after each venting–activation cycle as expected. The decrease of the H_2 sticking probability is found to depend on the heating temperature during activation: the higher the temperature the lower the loss. For activation cycles performed at 200 °C for 24 h the sticking probability decreases roughly as the inverse of the number of cycles; in this case the pumping speed can be partially recovered by increasing the heating temperature. On the other hand, activations carried out at 300 °C leads to a reduction of the H_2 sticking probability of a factor of two after about 30 cycles.

The loss of performance recorded along the first 10 cycles does not depend on the thickness of the film in the range $0.25 \div 5$ μm although an abrupt reduction of the pumping speed is observed for the thinnest (0.25 μm) coating after about 12 cycles when heating at 200 °C [47].

The experimental results can be interpreted by using both thermodynamic and kinetic considerations. Each cycle dissolves into the film an identical quantity of oxygen; hence the maximum possible number of cycles is reached when the oxygen solubility limit is attained. If an oxygen solubility limit similar to that of the elements of the fourth group is considered, full saturation after about 100 cycles is expected for each μm of

film thickness [47]. However, heating at temperatures lower than 250 °C does not allow a uniform oxygen concentration to be reached in the film and, as a consequence, oxygen atoms are settled in the film to form a concentration profile with the maximum close to the surface, which finally leads to accelerated performance degradation. These conclusions are not peculiar to films but rather they apply to NEG materials of any nature.

The film degradation can be also explained in terms of C accumulation on the surface; in effect this element needs a higher heating temperature to be dissolved in the film bulk [48–50]. The two models are going to be tested by performing activation–venting cycles of coatings of different roughness.

4. Production of Ti–Zr–V coated vacuum chambers for the LHC

The Large Hadron Collider (LHC), due to start operation in 2007, is a particle accelerator that will ultimately collide beams of protons at energy of 14 TeV. Its main ring (27 Km in length) is composed of arcs where superconducting magnets bend the beams and long straight sections (LSS) where the two beams collide or where beam acceleration, injection, extraction and monitoring are placed. The LSS are composed of about 6 km of beam pipes (about 1200 vacuum chambers) and, to provide distributed pumping and low SEY, they are going to be almost all Ti–Zr–V coated.

The LSS vacuum chambers are made of several materials (bare or copper plated stainless steel, aluminium, beryllium, OFS and OFE copper, copper plated mumetal) and they have disparate sizes (cylindrical and conical symmetry, circular or elliptical cross-section, length varying between 20 cm to 7 m, diameter ranging between 30 to 450 mm). A key point for the success of this operation is the chemical treatment of the substrate materials before coating; in particular for the case of extruded copper tubes the cortical layer (about 50 μm) has to be chemically removed. An inadequate surface treatment leads to NEG film deterioration and, in the worst case, peel-off.

The coating production planning has to fit the ring installation planning, which has fixed the conclusion of the vacuum system assembling by end of 2006. To face the tight schedule a dedicated facility was built at CERN. It consists of three cylindrical magnetron sputtering systems that allow coating vacuum chambers with a maximum length of about 7.5 m and maximum diameter of about 60 cm. Each unit consists of a vacuum pumping system, a manifold, a base support and a vertical solenoid (see Fig. 2). The chambers are assembled on a special cradle which is able to support up to four chambers if their diameter is less than 100 mm. A 16 m long assembling bench allows the horizontal insertion of the cathodes in the chambers. The whole structure can then be lifted up with a crane and inserted into the solenoid, installed inside a 6.3 m deep pit.

In the simplest geometrical configuration, the three-wire cathode is inserted in the chamber and aligned along the pipe main axis. For more complicate structure, more than one cathode is necessary to guarantee uniform film thickness. As an example for chambers whose cross-section is elliptical, at least two cathodes are inserted. In another case, where two pipes converge into one (the recombination chambers), three cathodes are necessary to coat the three branches of the vacuum chamber. In special cases the cathode is mechanically deformed to match the chamber profile.

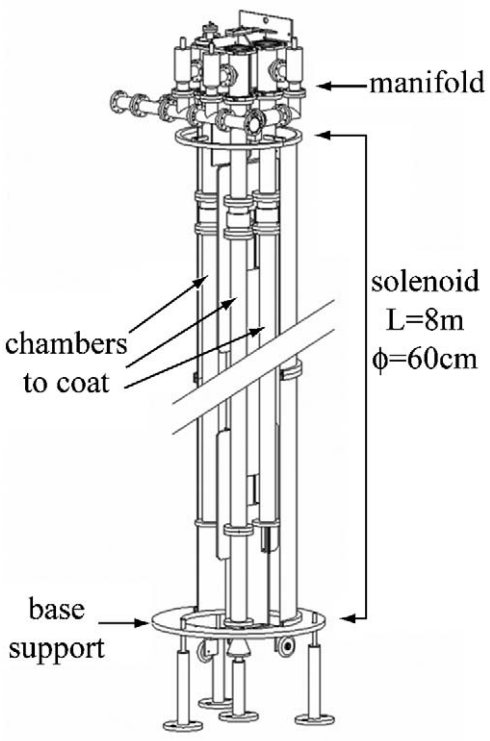

Fig. 2. Drawing of the set-up used for the coating of the LHC-LSS vacuum chambers. Three such units are available at CERN.

The vacuum pumping system, equipped with a turbomolecular pumping unit, cold cathode gauges, and a residual gas analyzer, is installed on a platform located at the top of the solenoid and is connected to the manifold by a bellow. The chambers are baked at 200 °C overnight before coating.

The supports and electrical feedthroughs for the cathodes are located on top of the manifold and are fed by 1.5 kW DC plasma power supplies (one per cathode). The solenoids are 8 m long and provide magnetic field up to 300 G. One of the solenoid offers the possibility of coating independently chamber sections 1.33 m in length allowing a better uniformity of the film thickness in long conical chambers. Ion current densities range from 0.06 to 0.19 Am^{-1}, (depending on cathode wire's diameter), for a potential of −500 V.

During the coating process the chamber's temperature is kept at 100 °C. As shown in Fig. 1, coating at 250 °C would have increased the surface roughness and the pumping performances. However, the total coated surface in the LSS is so large that the saturation of the film should not be a critical item. In addition, a rougher film surface could have an accelerated ageing due to the higher quantity of oxygen dissolved after each air venting–activation cycle.

The discharge gas is Kr, which is injected at a pressure of about 10^{-2} Torr. After coating, the chambers are dry air

vented, dismounted from the cradle, pumped, filled with dry nitrogen at 1.2 bar and finally tightly stored. An average production rate of about 20 chambers per week is guaranteed.

To assure the quality of the production, after every run the elemental composition is checked by EDX on a copper sample coated simultaneously with one of the chambers. This sample will also be used for thickness measurement by electron microscopy. A similar sample will be used to evaluate the activation behaviour by XPS. The pumping speed performance of the NEG film is evaluated every week by measuring two 25 cm long tubes coated together with the chambers and, once per month of production, one chamber is fully characterized (pumping speed, surface capacity, CH_4 and Kr outgassing).

5. Conclusions

NEG film coatings that can be activated at temperatures compatible with most of the structural materials used in UHV applications were obtained by simultaneous sputtering of Ti, Zr and V. The favourable activation properties are correlated with nanometric grain size. After activation, the Ti–Zr–V film coated on the whole inner surface of vacuum chambers assures distributed pumping and, due to its clean surface, low particle induced desorption yields and secondary electron yield. These benefits provide an ideal application of Ti–Zr–V coatings in the vacuum systems of particle accelerators. In the LHC, the next CERN particle accelerator, this pumping solution will be extensively applied in the 6 km of the long straight sections. In order to comply with the installation planning, a dedicated sputtering system is now operational and produces in average 20 vacuum chambers per week.

The commissioning and the operation of the LHC will provide additional data on the behaviour of this pumping technology, which will be useful for all the vacuum and accelerators community.

Acknowledgements

We are indebted with Cristoforo Benvenuti who is at the origin of all the work present in this paper.

This work wouldn't have been possible without the enthusiasm and the skill of many CERN colleagues; in particular those in charge of the following services: coating, assembling, drawing office, surface cleaning, metallurgical and surface analysis.

References

[1] C. Benvenuti, Proceedings of EPAC, 1998, CERN Library URL: http://accelconf.web.cern.ch/AccelConf/e98/PAPERS/THZ02A.PDF.
[2] C. Benvenuti, R. Calder, O. Gröbner, Vacuum 37 (1987) 699.
[3] PEP-Conceptual Design Report, LBL-4288/SLAC-189 (1976).
[4] C. Benvenuti, Nucl. Instrum. Methods 205 (1983) 391.
[5] A. Prodromides, Ph.D Thesis No. 2652 (2002), Faculté Sciences de Base, Section de Physique, EPFL; and references therein. CERN Library URL: http://documents.cern.ch/cgibin/setlink?base=preprint&categ=cern&id=cern-thesis-2002-042.
[6] Landolt-Börnstein Numerical Data and Functional Relationships in Science and Technology, Volume 5, Editor: O. Madelung, Springer-Verlag.
[7] V.V. Vykhodets, S.M. Klotsman, T.T.Ye. Kurennykh, A.D. Levin, Phys. Met. Metallogr. 68 (1989) 145.
[8] C. Benvenuti, P. Chiggiato, F. Cicoira, Y. L'Aminot, J. Vac. Sci. Technol., A 16 (1998) 148.
[9] A. Prodromides, C. Scheuerleine, M. Taborelli, Vacuum 60 (2001) 35.
[10] C. Benvenuti, J.M. Cazeneuve, P. Chiggiato, F. Cicoira, A. Escudeiro Santana, V. Johanek, V. Ruzinov, J. Fraxedas, Vacuum 53 (1999) 219.
[11] C. Benvenuti, P. Chiggiato, P. Costa Pinto, A. Escudeiro Santana, T. Hedley, A. Mongelluzzo, V. Ruzinov, I. Wevers, Vacuum 60 (2001) 57.
[12] P. Chiggiato, R. Kersevan, Vacuum 60 (2001) 67.
[13] S.W. Zang, et al., Proceedings of EPAC, 2004, CERN Library URL: http://accelconf.web.cern.ch/AccelConf/e04/PAPERS/MOPLT178.PDF.
[14] R. Kersevan, Proceeding of EPAC, 2002, CERN Library URL: http://accelconf.web.cern.ch/AccelConf/e02/PAPERS/WEPDO029.pdf.
[15] C. Benvenuti, N. Circelli, M. Hauer, Appl. Phys. Lett. 45 (1984) 583.
[16] C. Benvenuti, S. Calatroni, P. Darriulat, M. Peck, A.-M. Valente, C. Van't Hof, Physica C 351 (2001) 421.
[17] A. Prodromides, C. Scheuerlein, M. Taborelli, Vacuum 60 (2001) 35.
[18] M. Lozano, J. Fraxedas, Surf. Interface Anal. 30 (2000) 623.
[19] V. Matolin, V. Dudr, S. Fabik, V. Chab, K. Masek, I. Matolinova, K.C. Prince, T. Skala, F. Sutara, N. Tsud, K. Veltruska, Appl. Surf. Sci. 243 (2005) 106.
[20] S. Fabik, V. Chab, V. Dudr, K. Masek, K.C. Prince, F. Sutara, K. Veltruska, N. Tsud, M. Vondracek, V. Matolin, Surf. Sci. 566–568 (2004) 1246.
[21] C. Benvenuti, P. Chiggiato, A. Mongelluzzo, A. Prodromides, V. Ruzinov, C. Scheuerlein, M. Taborelli, F. Lévy, J. Vac. Sci. Technol., A 19 (2001) 2925.
[22] C. Benvenuti, P. Chiggiato, P. Costa Pinto, A. Prodromides, V. Ruzinov, Vacuum 71 (2003) 307.
[23] S. Calatroni, E. Barbero-Soto, C. Benvenuti, L. Ferreira, H. Neupert, CERN internal note CERN-TS-2004-003(MME); CERN Library URL: https://edms.cern.ch/file/521090/1/CERN-TS-2004-003(MME).pdf.
[24] B. Window, J. Vac. Sci. Technol., A 11 (1993) 1522 (and references therein).
[25] S. Amorosi, M. Anderle, C. Benvenuti, S. Calatroni, J. Carver, P. Chiggiato, H. Neupert, W. Vollenberg, Vacuum 60 (2001) 89.
[26] H.F. Winters, E. Kay, J. Appl. Phys. 38 (1967) 2938.
[27] H.F. Winters, E. Kay, J. Appl. Phys. 43 (1972) 789.
[28] A.V. Walker, D.A. King, J. Chem. Phys. 112 (2000) 4739.
[29] D.T.P. Watson, J. van Dijk, J.J.W. Harris, D.A. King, Surf. Sci. 506 (2002) 243.
[30] A.C. Luntz, H.F. Winters, J. Chem. Phys. 101 (1994) 980.
[31] C. Benvenuti, F. Francia, J. Vac. Sci. Technol., A 6 (1988) 2528.
[32] C. Benvenuti, F. Francia, J. Vac. Sci. Technol., A 8 (1990) 3864.
[33] E. Fromm, O. Mayer, Surf. Sci. 74 (1978) 259.
[34] P. Chiggiato and C. Bellachioma, Water vapour pumping speed of Ti–Zr–V films, EST-SM-DA internal note, 3-2003/P.C.
[35] J.S. Ford, P.J. Goddard, R.M. Lambert, Surf. Sci. 94 (1980) 339; G.A. Somorjai, Chemistry in Two Dimensions, Cornell University Press, 1981, p. 268.
[36] C. Benvenuti, A. Escudeiro Santana, V. Ruzinov, Vacuum 60 (2001) 279.
[37] P. Chiggiato, G. Chuste, P. Costa Pinto, I. Wevers, unpublished, to be submitted to J. Vac. Sci. Technol.
[38] P. Chiggiato, S. Clair, I. Wevers, The Sieverts' law of Ti–Zr–V coatings, EST-SM-DA internal note, 02-2000/P.C.
[39] O. Gröbner, CAS — Proceedings of the CERN Accelerator School: Vacuum Technology, 1999, p. 127, CERN Library URL: http://doc.cern.ch//archive/cernrep//1999/99-05/p127.pdf.
[40] P. Chiggiato, J.M. Cazeneuve, V. Johanek, Effect of re-pumping by NEG coatings on the reduction of the desorption yields measured by the ESD system: a Monte Carlo based simulation. EST-SM-DA internal note 05-1998/P.C.
[41] I.R. Collins, V. Ruzinov, O.B. Malyshev, V. Anashin, R. Dostovalov, N. Fedorov, A. Krashov, Proceedings of EPAC, 2002, CERN Library URL: http://accelconf.web.cern.ch/AccelConf/e02.

[42] Anashin, et al., Vacuum 75 (2004) 155.
[43] E. Mahner, J. Hansen, D. Küchler, M. Malabaila, M. Taborelli, Phys. Rev. Spec. Top., Accel. Beams 8 (2005) 053201.
[44] G. Arduini, et al., Proceedings of EPAC, 2000, CERN Library URL: http://accelconf.web.cern.ch/AccelConf/e00/PAPERS/TUOAF101.pdf.
[45] B. Henrist, N. Hilleret, C. Scheuerlein, M. Taborelli, App. Surf. Sci. 172 (2001) 95.
[46] G. Arduini, et al., Proceedings of EPAC, 2004, CERN Library URL: http://accelconf.web.cern.ch/AccelConf/e04/PAPERS/WEPLT044.PDF.
[47] P. Chiggiato, G. Chuste, P. Costa Pinto, I. Wevers, unpublished, to be submitted to J. Vac. Sci. Technol. A.
[48] C. Scheuerlein, M. Taborelli, J. Vac. Sci. Technol., A 20 (2002) 93.
[49] C. Scheuerlein, Master of Science Thesis, Department of Material Engineering, University of Surrey, 2002, CERN library URL: http://doc.cern.ch/archive/electronic/cern/preprints/thesis/thesis-2002-026.pdf.
[50] V. Matolin, K. Masek, I. Matolinova, T. Skala, K. Veltruska, App. Surf. Sci. 235 (2004) 202.
[51] V. Baglin, personal communication, talk presented at IVC-15, St. Francisco (USA), 2001.